Lubricant effect of copper nanoclusters on the dislocation core in α-Fe

Zhengzheng Chen,[1] Nicholas Kioussis,[1] Nasr Ghoniem,[2] and Tadashi Hasebe[3]
[1]*Department of Physics, California State University, Northridge, California 91330-8268, USA*
[2]*Department of Mechanical and Aerospace Engineering, UCLA, Los Angeles, California 90095-1597, USA*
[3]*Department of Mechanical Engineering, Kobe University, 1-1 Rokkodai, Nada, Kobe 657-8501, Japan*
(Received 22 August 2007; revised manuscript received 22 October 2007; published 18 January 2008)

Ab initio based calculations reveal that Cu nanoclusters in α-Fe dramatically alter the core structure of a screw dislocation from nonpolarized in pure Fe to polarized. Complementary corroborative atomistic simulations using empirical interatomic potentials reveal that the Cu nanoprecipitate substantially enhances the edge component, which is in agreement with experiment. The core path under shear stress exhibits a stable $\rightarrow$ metastable $\rightarrow$ stable transition. In contrast, Cr clusters do not change the core polarization and increase the Peierls stress, thus hardening Fe. The origin in electronic structure of the Cu lubricant effect in facilitating the shear of atomic rows and the contrasting effects of Cu and Cr is elucidated.

DOI: 10.1103/PhysRevB.77.014103 PACS number(s): 61.72.Lk, 71.15.−m, 62.20.F−

I. INTRODUCTION

Plastic deformation of body-centered-cubic (bcc) metals is mainly controlled by the intrinsic core properties of $a/2\langle 111\rangle$ screw dislocations. Unlike the highly mobile edge dislocations, the motion of screw dislocations is restricted by a nonplanar atomic core structure. This, in turn, results in low mobility, thermal-activated formation and migration of kink pairs, and a low-temperature ($T<0.2T_{melt}$, where T_{melt} is the melting temperature) dependent yield stress.

The ubiquitous presence of solute atoms in bcc metals and the resultant dislocation-solute atom or -precipitate interactions are of central interest since they are key to understanding solid solution hardening (SSH), where solutes serve as obstacles to dislocation motion. On the other hand, extensive experimental studies[1] in bcc alloys have provided clear evidence of the opposite effect, the so-called solid solution softening (SSS). In the SSS phenomenon, the effect of alloying decreases the yield strength at low temperatures and low impurity concentrations. These observations clearly suggest that another contribution to dislocation mobility stems from a rather strong sensitivity to trace amounts of substitutional and/or interstitial impurities, the origin of which has not yet been clarified.[2] The intrinsic mechanisms of SSS have been attributed to mismatch in size and in shear moduli between solute and matrix atoms. However, recently, the *chemical* or *electronic* mechanism on both the kink formation and migration rates in Mo has been shown to play an important role.[3,4]

The α-Fe-X base alloys (X=Cr,Cu,Ni, etc.) are ideal systems to study SSH due to the very low solubility of X in Fe at low temperatures and the importance of solute precipitation on the irradiation hardening and embrittlement of low alloy reactor pressure vessel steels.[1,2] Previously, studies based on empirical interatomic potentials were used to study precipitate interactions in Fe-Cu and have shown that $\sim$3 nm Cu precipitates strengthen α-Fe.[2,5,6] However, the origin of the electronic structure responsible for the SSS or SSH in α-Fe remains an unexplored area thus far[7] because of the inadequacy of empirical potentials.

The purpose of this work is to present a theoretical study of the effect of Cu or Cr solutes and solute clusters on the dislocation core properties of the $a/2\langle 111\rangle$ screw dislocation in α-Fe. We employ an *ab initio* based approach whose results are corroborated by complementary atomistic simulations using empirical interatomic potentials. The calculations reveal that Cu nanoprecipitates induce a dramatic change in the core structure from nonpolarized in pure Fe to polarized. In sharp contrast, it will be shown that Cr precipitates have small effect on the core polarization and increase the Peierls stress (σ_P). The underlying atomistic mechanism responsible for these uniquely electronic structure effects will be elucidated here.

The next section gives a brief description of the two theoretical methods used in our study. In Sec. III, we present the results of the electronic structure and the dislocation core configurations in pure Fe, Fe-Cu, and Fe-Cr systems. Finally, we give a brief summary in Sec. IV.

II. THEORETICAL METHOD

Ab initio calculations of dislocations and dislocation-solute interactions, even though most accurate, are computationally expensive. As a result, most atomistic simulations are based on empirical descriptions of atomic interactions. However, such approaches depend critically on the interatomic potentials which are determined by fitting to experimental or *ab initio* data, and hence they are limited to describing accurately the effects of alloying. The hybrid *ab initio* based approach of the atomic-row (AR) model of Suzuki[9] for a screw dislocation in bcc metals offers a plausible alternative. It serves as a link between *ab initio* and atomistic approaches and represents a compromise between computationally efficiency and accuracy. The inter-row potential (IRP), derived from *ab initio* calculations, allows the treatment of solutes in the core, while the dislocation core structure is determined by relaxing the ARs using the IRP,[4] similar to atomistic simulations employing interatomic interactions.

The IRP, $\Phi^{(\text{Fe-}X)}(\tilde{u})$, between two ARs consisting of Fe and X (X=Fe,Cu,Cr) atoms, respectively, is assumed to depend only on the relative displacement $\tilde{u}$ of the ARs along the dislocation line and is of the form[9]

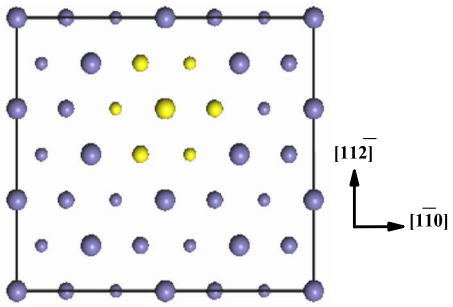

FIG. 1. (Color online) ⟨111⟩ projection of the supercell used for the calculation of $\Delta E^{(\text{Fe-}X)}$. The different circle sizes denote atoms on three successive (111) layers. The Fe atoms are denoted by blue (dark gray) and the solute atoms are denoted by yellow (light gray).

$$\Phi^{(\text{Fe-}X)}(\tilde{u}) = \frac{\Phi_0^{(\text{Fe-}X)}}{[1-4\alpha^{(\text{Fe-}X)}]}\left[\cos 2\pi\tilde{u} - \alpha^{(\text{Fe-}X)}\cos 4\pi\tilde{u} + \frac{1}{2}[1-\alpha^{(\text{Fe-}X)}]\right]. \quad (1)$$

Here, $\tilde{u}=u/b$, where u is the relative displacement and b is the Burgers vector. The parameters $\Phi_0^{(\text{Fe-}X)}$ and $\alpha^{(\text{Fe-}X)}$ are determined from *ab initio* calculations. Note that the IRP approach neglects the edge component of the displacement field, which is important for the core structure, mobility, and kink nucleation.[10] The change in energy, $\Delta E^{(\text{Fe-}X)}(\tilde{u})$, per unit length to displace an AR of X atoms in the core along ⟨111⟩ relative to a nearest-neighbor (NN) Fe atomic row,

$$\Delta E^{(\text{Fe-}X)}(\tilde{u}) = 3[\Phi^{(\text{Fe-}X)}(\tilde{u}-1/3) + \Phi^{(\text{Fe-}X)}(\tilde{u}+1/3)], \quad (2)$$

can be evaluated by *ab initio* calculations. The parameters $\Phi_0^{(\text{Fe-}X)}$ and $\alpha^{(\text{Fe-}X)}$ can then be determined from Eqs. (1) and (2). The change of inter-row energy has been recently used to study the SSS or SSH in Mo when solute atoms are substituted into that row.[3]

Spin-polarized *ab initio* calculations were carried out using the VASP code.[11,12] The supercell, shown in Fig. 1, consists of three atomic layers in the ⟨111⟩ direction and 12 atoms per layer. The ARs are along ⟨111⟩ each represented by a circle. We have used a $4\times4\times8$ k mesh according to the Monkhorst-Pack scheme.[13] The generalized gradient approximation functional[14] is used to treat the exchange and correlation potential. The Fe-X IRP is determined by substituting one atomic row, denoted by yellow in Fig. 1, with the X solute. For the X-X IRP, we substitute the central AR and its six NN rows, denoted by yellow, with solute atoms.

In order to model a dislocation using the *ab initio* based IRP approach, a $a/2\langle111\rangle$ screw dislocation is placed at the center of a rectangular cell of $101.4\times87.8\times2.48$ Å^3 along the ⟨110⟩, ⟨112⟩, and ⟨111⟩ directions, respectively. The slab contains 1875 ARs with a periodic length of $1b$ along the dislocation line. The displacements of the two outermost boundary rows of the slab along the ⟨110⟩ and ⟨112⟩ directions are held fixed to the elastic solution values during the relaxation process. The initial geometry for the dislocation in pure Fe is the displacement field $\{u_i\}$ from isotropic elasticity

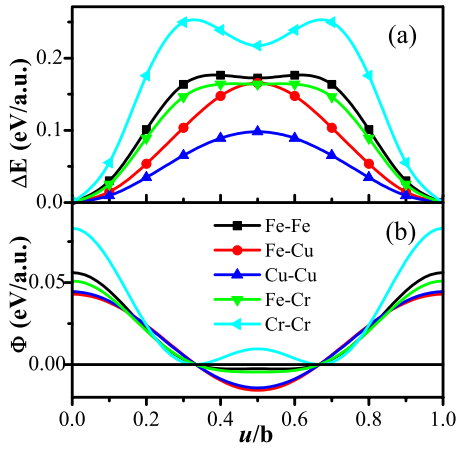

FIG. 2. (Color online) (a) Energy change per unit length, $\Delta E^{(\text{Fe-}X)}$ and $\Delta E^{(X\text{-}X)}$ for X=Fe, Cu, and Cr, versus the normalized AR displacement u/b along ⟨111⟩. (b) Corresponding variation of IRP, $\Phi^{\text{Fe-}X}$ and $\Phi^{X\text{-}X}$.

theory, which is adequate for bcc Fe (nearly isotropic). Atomic row positions are, in turn, relaxed by minimizing the total energy,

$$E_{tot} = \frac{1}{2}\sum_{i,j,i\neq j}\Phi^{(\text{Fe-}X)}(u_i - u_j), \quad (3)$$

using the conjugate gradient approach. Here, the sum is only over NN ARs.

III. RESULTS AND DISCUSSION

Figure 2(a) shows $\Delta E^{(\text{Fe-}X)}$ and $\Delta E^{(X\text{-}X)}$ versus $\tilde{u}$ for X =Fe, Cu, and Cr. The corresponding IRP, $\Phi^{\text{Fe-}X}$ and $\Phi^{X\text{-}X}$ versus $\tilde{u}$ are shown in Fig. 2(b). For Fe-Fe, Fe-Cr, and Cr-Cr, ΔE exhibits two well-pronounced maxima at $u=\frac{b}{3}$ and $u=\frac{2b}{3}$ associated with both the bcc structure and the unfilled $3d$ band for Fe and the solute atom. On the other hand, Cu solutes reduce dramatically the atomic-row shear energies for the Fe-Cu and Cu-Cu rows. Moreover, there is a change of the shape of ΔE, which displays a single maximum at $u=\frac{b}{2}$ for both Fe-Cu and Cu-Cu. These results clearly demonstrate that Cu solutes act as lubricants and facilitate the shear process between the Fe-Cu and Cu-Cu rows. Analysis of the density of states and charge density indicate that the NN inter-row interaction for Fe-Fe, Fe-Cr, and Cr-Cr is dominated by t_{2g}-t_{2g} hybridization at the Fermi energy. The stronger bonding between NN Cr pairs compared to Fe pairs results in $\Delta E^{(\text{Cr-Cr})} > \Delta E^{(\text{Fe-Fe})}$. On the contrary, the Fe-Cu and Cu-Cu NN inter-row interactions are dominated by t_{2g}-s hybridization, which being weaker than the t_{2g}-t_{2g}, results in smaller $\Delta E^{(\text{Fe-Cu})}$.

In Fig. 3(a), we show the relaxed dislocation core structure for pure Fe employing the differential displacement (DD) maps[10,15] for the screw component using the *ab initio* based IRP approach. The arrows indicate the relative ⟨111⟩ displacement of neighboring atoms produced by the dislocation. The length of the arrow is proportional to the magnitude

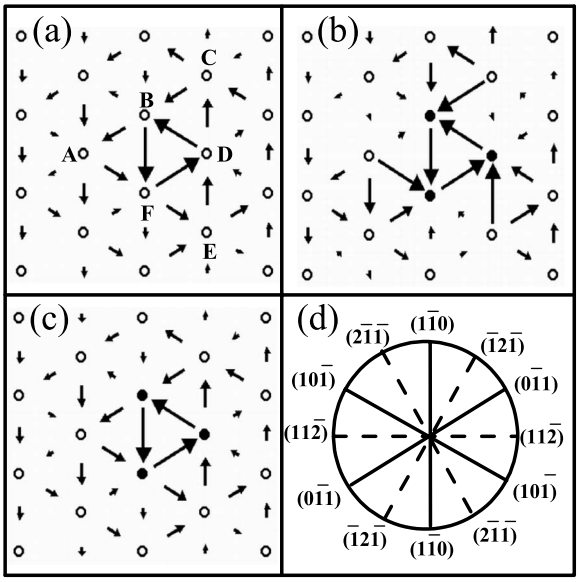

FIG. 3. DD map of the core for a $a/2\langle 111\rangle$ screw dislocation in (a) pure Fe, (b) Fe-Cu, and (c) Fe-Cr, calculated from the *ab initio* based IRP approach. The hollow circles and solid circles represent Fe and impurity atoms, respectively. (d) [111] stereographic projection of all {110} and {112} planes belonging to the [111] zone.

of the displacement difference and the direction of the arrow indicates the sign of the displacement difference. When the arrow touches the centers of the two atoms, their relative displacement is $b/3$. The orientation of all the {110} and {112} planes belonging to the [111] zone is shown in Fig. 3(b). The dislocation core for pure Fe is symmetric (nondegenerate) and spreads symmetrically on the six planes, in agreement with recent fully *ab initio*[16] and atomistic[17] calculations. The core structure for a small Cu cluster composed of three rows along the dislocation core, as shown in Fig. 3(b), changes dramatically from symmetric to nonsymmetric (degenerate), where the dislocation core spreads primarily into three {110} planes. Thus, the 2.5 Å size Cu cluster reduces the core nonplanarity and renders it to more planar. In sharp contrast, the three atomic row Cr precipitate in Fig. 3(c) has a very small effect on the core structure, i.e., the core remains isotropic as in the case of pure Fe.

The change of the core structure induced by the Cu nanoprecipitate invites the question what is the core structure of the $a/2\langle 111\rangle$ screw dislocation in pure bcc Cu, with lattice constant of $a_0=2.866$ Å. The core structure of the screw dislocation in bcc Cu calculated from the *ab initio* based IRP method and the Finnis-Sinclair (FS) interatomic potential[23] is shown in Figs. 4(a) and 4(b), respectively. Interestingly, both approaches yield a nonsymmetric (degenerate) core structure, similar to that of the Cu nanoprecipitate in pure Fe, indicating that the unique inter-row energy profile between Cu atomic rows in Fig. 2 is responsible for the more planar core structure.

To quantify the effect of chemistry on the core structure of Fe, we have calculated the core polarization p,[18]

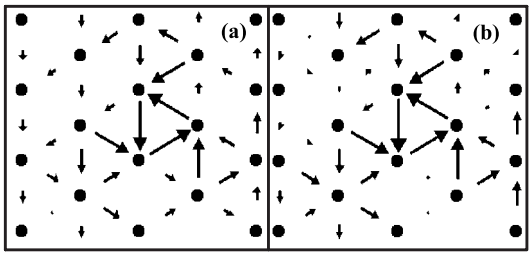

FIG. 4. DD map for the core structure for a $a/2\langle 111\rangle$ screw dislocation in pure bcc Cu using the (a) *ab initio* based IRP approach and (b) the FS potential.

$$p = \frac{|d_{AB} - d_{BC}| + |d_{CD} - d_{DE}| + |d_{EF} - d_{FA}|}{b}. \quad (4)$$

Here, $d_{i,j}$, (i,j=A, B, C, D, E, or F) is the relative displacement between two neighboring atoms in the two columns denoted as i and j in Fig. 3(a). Thus, a symmetric core leads to $p=0$, while $p=1$ corresponds to a fully asymmetric core. In Table I, we list the polarization of the dislocation core as a function of the number of solute ARs. The polarization increases with increasing Cu concentration, indicating that the Cu-Cu NN atomic pairs play a significant role on the dislocation core, as pointed out empirically by Tapasa *et al.*[19] On the other hand, the polarization is almost independent of the Cr concentration, as is also evident in Fig. 3(c). It is important to emphasize that due to the small size of the solute precipitate, the change of polarization induced by Cu cannot be attributed to the elastic modulus mismatch between Cu and Fe. Rather, it is purely a "chemistry effect" whose origin lies in the different (similar) electronic structure between Cu (Cr) and Fe, and the change of $3d$-$3d$ hybridization in pure Fe or Fe-Cr system to the $3d$-$4s$ hybridization in the Fe-Cu system. One should expect a similar effect with other simple-metal alloying elements.

Since the core polarization is a controlling factor of dislocation mobility,[10,20] one would expect that under external stress, the polarized core in Fe-Cu will behave differently from the nonpolarized one in pure Fe. In order to corroborate the results of the *ab initio* based inter-row approach and to study the effect of external stress, we have carried out also static atomistic simulations at zero temperature based on the embedded atom method. Moreover, the atomistic simulations include atomic displacements perpendicular to $\langle 111\rangle$ (edge component), which even though small, they are important in kink formation and in decrease in σ_P.[10] We have employed the interatomic potentials in Ref. 22 for pure Fe, and in Ref.

TABLE I. Polarization p of the screw dislocation core, defined in Eq. (4), as a function of the number of solute AR using the *ab initio* IRP approach.

	No. impurity atoms	0	1	2	3
p	Cu	0.00	0.11	0.48	0.99
	Cr	0.00	0.01	0.02	0.00

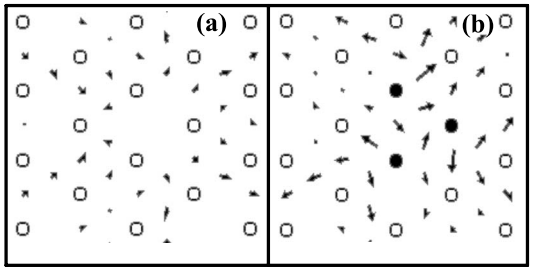

FIG. 5. DD map of the edge component of the dislocation core for (a) pure Fe and (b) Fe-Cu using the atomistic simulations based on the FS potential. The vectors have been magnified by a factor of 5 to make them clearly visible.

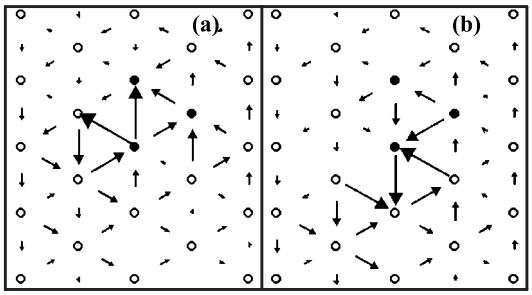

FIG. 6. DD map of the screw dislocation core for Fe-Cu under pure shear stress of (a) 0.8 GPa, and (b) 1.5 GPa, respectively by using EAM. The atomic notation is the same as in Fig. 4.

23 for the Fe-Cu and for Cu-Cu interactions. The dimensions of the supercell are $13\times20\times3$ nm^3, and the system consists of approximately 64 800 atoms. Interestingly, the interatomic potentials of Refs. 22 and 23 give a nonpolarized (symmetric) dislocation core for pure Fe and a fully polarized (asymmetric) core for the three AR Cu precipitate, both in excellent agreement with our results using the IRP approach. We find that the Cu nanocluster *enhances* substantially the edge component of the dislocation, as shown in Fig. 5, suggesting that it may facilitate kink nucleation, which is in agreement with experiment.[8] However, three-dimensional simulations, currently under study, are necessary to confirm our conjecture of the Cu-induced facilitation of kink formation in Cu nanoprecipitates of small diameters (<1 nm). The nonglide stress (Escaig stress) is defined as the edge component of the diagonal stress tensor interacting only with the edge component of the dislocation displacement field.[10,21] Consequently, since the Cu nanoprecipitate enhances the edge component, the nonglide shear stress will have a larger effect on the core structure and the cross-slip properties in Fe-Cu alloys, in contrast to pure Fe.

Next, using the FS atomistic potentials, we examine the glide paths of the core for an applied pure glide shear stress on the $(1\bar{1}0)$ plane in the $\langle 111\rangle$ direction. We increase the stress incrementally and relax the configuration between each increment. σ_P for pure Fe is 1.2 GPa and is well defined. Namely, below this critical stress the dislocation is stable, and above which the core moves.

In sharp contrast, there are two critical stresses for the Cu precipitate. The dislocation core structures for these two critical stress values of 0.8 GPa and 1.5 GPa are shown in Figs. 6(a) and 6(b), respectively. When the applied stress reaches 0.8 GPa, the dislocation moves by one atomic distance and exhibits a *split* core which is *metastable*. This metastable configuration remains fixed until the second upper critical stress of 1.5 GPa is reached, above which the motion becomes unbounded, i.e., the Cu cluster induces a stable $\rightarrow$ metastable $\rightarrow$ stable transition for the dislocation core under external stress. The IRP approach for the Fe-Cu system gives similar results as the atomistic simulations using the FS potential, but with different values of the critical stresses, listed in Table II. A similar behavior for the existence of two critical stresses was found in pure Fe in Ref. 24 using the potential developed by Simonelli *et al.*[25] It is interesting to note that σ_P for pure Fe lies between the upper and lower values of the critical stress for the Cu precipitate, and the upper value agrees with a recent estimate.[5] This result indicates that the nanocluster cylindrical Cu precipitate strengthens α-Fe. However, the strengthening mechanism is more complex, involving a two-step change of the dislocation mobility, with the Peierls stress of the second step being higher than that of pure Fe.

There are several available FS interatomic potentials for Fe-Cr.[26–33] Here, we use that developed by Olsson *et al.*[26] because of its compatibility with the potential of Ackland *et al.* for pure α-Fe.[22] The result shows that the critical shear stress to move the dislocation core on the {110} plane in the Fe-Cr system is also well defined and unique, but with the value of 2.0 GPa, which is 67% higher than that in pure α-Fe. For comparison, we also list in Table II the result of σ_P using the IRP method, which is consistent with the FS calculation. Thus, our results indicate that the SSH effect of Cr clusters is due to the fact that they serve as obstacles for dislocation motion due to the strong bonding of Cr pairs or clusters, consistent with the interatomic results of Wallenius *et al.*[28]

IV. CONCLUSION

In summary, using an *ab initio* based approach, we find that Cu clusters change dramatically the core structure of a

TABLE II. Values of critical stress (σ_P) in GPa using the IRP methods and the FS potential, respectively. The lower and upper values of σ_P^l and σ_P^u for the Fe-Cu system are explained in the text.

	Pure Fe	Fe-Cu (σ_P^l)	Fe-Cu (σ_P^u)	Fe-Cr	Pure Cr	bcc Cu
IRP	1.6	1.3	1.9	1.8	2.1	1.8
FS	1.2	0.8	1.5	2.0	2.3	1.7

screw dislocation from nonpolarized in pure Fe to polarized. These results are corroborated by atomistic simulations indicating that Cu facilitates the core planarity and enhances substantially the edge component. The core path under pure glide shear stress exhibits a stable→metastable→stable transition. The Peierls stress for pure Fe lies between the upper and lower values of the critical stress for the Cu precipitate. In sharp contrast, Cr solute clusters do not change the core polarization and increase σ_P, thus hardening Fe. The underlying atomic origin responsible for the unusual lubricant effect of Cu lies on the reduction of the Fe-Cu and Cu-Cu AR interactions which are dominated by the weak t_{2g}-s hybridization. On the other hand, the Fe-Cr and Cr-Cr AR interactions are dominated by the much stronger t_{2g}-t_{2g} hybridization.

ACKNOWLEDGMENTS

We acknowledge valuable discussions with Dallas R. Trinkle, M. Shehadeh, and B. Ramirez. This research was supported by DOE NERI Grant No. DE-FC07-06ID14748.

[1] E. Pink and R. J. Arsenault, Prog. Mater. Sci. **24**, 1 (1979).
[2] T. Harry and D. J. Bacon, Acta Mater. **50**, 195 (2002).
[3] D. R. Trinkle and C. Woodward, Science **310**, 1665 (2005).
[4] N. I. Medvedeva, Y. N. Gornostyrev, and A. J. Freeman, Phys. Rev. B **72**, 134107 (2005).
[5] T. Harry and D. J. Bacon, Acta Mater. **50**, 209 (2002).
[6] J. Marian, B. D. Wirth, R. Schaublin, G. R. Odette, and J. M. Perlado, J. Nucl. Mater. **323**, 181 (2003).
[7] H. Suzuki, in *Dislocations in Solids*, edited by F. R. N. Nabarro (North Holland, Amsterdam, 1979), Vol. 4, p. 193.
[8] S. K. Lahiri and M. E. Fine, Metall. Trans. **1**, 1495 (1970).
[9] H. Suzuki, in *Fundamental Aspects of Dislocation Theory*, edited by J. A. Simmons, R. deWitt, and R. Bullough (National Bureau of Standards, Washington, 1970), p. 253.
[10] M. S. Duesbery and V. Vitek, Acta Mater. **46**, 1481 (1998).
[11] P. E. Blöchl, Phys. Rev. B **50**, 17953 (1994).
[12] G. Kresse and J. Furthmuller, Phys. Rev. B **54**, 11169 (1996).
[13] H. J. Monkhorst and J. D. Pack, Phys. Rev. B **13**, 5188 (1976).
[14] J. P. Perdew, K. Burke, and M. Ernzerhof, Phys. Rev. Lett. **77**, 3865 (1996).
[15] V. Vitek, R. C. Perrin, and D. K. Bowen, Philos. Mag. **21**, 1049 (1970).
[16] S. L. Frederiksen and K. W. Jacobsen, Philos. Mag. **83**, 365 (2003).
[17] C. Domain and G. Monnet, Phys. Rev. Lett. **95**, 215506 (2005).
[18] G. Wang, A. Strachan, T. Çağin, and W. Goddard III, Phys. Rev. B **67**, 140101(R) (2003).
[19] K. Tapasa, D. J Bacon, and Y. N. Osetsky, Modell. Simul. Mater. Sci. Eng. **14**, 1153 (2006).
[20] V. Vitek, Cryst. Lattice Defects **5**, 1 (1974).
[21] V. Vitek, M. Mrovec, and J. L. Bassani, Mater. Sci. Eng., A **365**, 31 (2004).
[22] G. J. Ackland, M. I. Mendelev, D. J. Srolovitz, S. Han, and A. V. Barashev, J. Phys.: Condens. Matter **16**, S2629 (2004).
[23] G. J. Ackland, D. J. Bacon, A. f. Calder, and T. Harry, Philos. Mag. A **75**, 713 (1997).
[24] J. Chaussidon, M. Fivel, and D. Rodney, Acta Mater. **54**, 3407 (2006).
[25] G. Simonelli, R. Pasianot, and E. Savino, *Materials Theory and Modelling*, edited by J. Broughton, P. D. Bristowe, and J. M. Newsam, MRS Symposia Proceedings No. 291 (Materials Research Society, Pittsburgh, 1993), p. 567.
[26] P. Olsson, J. Wallenius, C. Domain, K. Nordlund, and L. Malerba, Phys. Rev. B **72**, 214119 (2005).
[27] D. Farkas, C. G. Schon, M. S. F. De Lima, and H. Goldenstein, Acta Mater. **44**, 409 (1996).
[28] J. Wallenius, P. Olsson, C. Lagerstedt, N. Sandberg, R. Chakarova, and V. Pontikis, Phys. Rev. B **69**, 094103 (2004).
[29] J. Shim, Y. Cho, S. Kwon, W. Kim, and B. Wirth, Appl. Phys. Lett. **90**, 021906 (2007).
[30] A. Caro, D. A. Crowson, and M. Caro, Phys. Rev. Lett. **95**, 075702 (2005).
[31] M. Yu. Lavrentiev, R. Drautz, D. Nguyen-Manh, T. P. C. Klaver, and S. L. Dudarev, Phys. Rev. B **75**, 014208 (2007).
[32] J. H. Shim, H. J. Lee, and B. D. Wirth, J. Nucl. Mater. **351**, 56 (2007).
[33] N. Juslin, K. Nordlund, J. Wallenius, and L. Malerba, Nucl. Instrum. Methods Phys. Res. B **255**, 75 (2007).